Sheffield Hallam University

New Measurement of the Direct 3α Decay from the 12C Hoyle State

SMITH, Robin, KOKALOVA, Tz, WHELDON, C, BISHOP, J. E., FREER, M, CURTIS, N and PARKER, D. J.

Available from Sheffield Hallam University Research Archive (SHURA) at:

http://shura.shu.ac.uk/16973/

Published version

Repository use policy

New Measurement of the Direct 3α Decay from the ^{12}C Hoyle State

R. Smith,[*] Tz. Kokalova,[†] C. Wheldon, J. E. Bishop, M. Freer, N. Curtis, and D. J. Parker

School of Physics and Astronomy, University of Birmingham, Edgbaston, Birmingham, B15 2TT, United Kingdom

Excited states in certain atomic nuclei possess an unusual structure, where the dominant degrees of freedom are those of α clusters rather than individual nucleons. It has been proposed that the diffuse 3α system of the ^{12}C Hoyle state may behave like a Bose-Einstein condensate, where the α clusters maintain their bosonic identities. By measuring the decay of the Hoyle state into three α particles, we obtained an upper limit for the rare direct 3α decay branch of 0.047%. This value is now at a level comparable with theoretical predictions and could be a sensitive probe of the structure of this state.

Because of its exceptionally high binding energy per nucleon, the helium nucleus (α particle) is thought to form inside the nucleus and propagate relatively unperturbed for a significant time [1]. In the most extreme case, one could imagine a nuclear state, which exists entirely as a system of interacting α particles, where the degrees of freedom of individual nucleons are no longer important [2].

Owing to its role in stellar helium burning, the ^{12}C Hoyle state resonance is considered an ideal candidate for such α-clustering phenomena. In the temperature range of 10^8–10^9 K, ^{12}C is produced through the triple-α process [3]. Sir Fred Hoyle recognized the need for a 0^+ resonance near to the 3α threshold to boost the capture process in order to account for the abundance of ^{12}C in the universe [4].

Despite experimental efforts [5], the structure of the Hoyle state has not been well elucidated. Algebraic cluster models assuming an equilateral triangle structure with $\mathcal{D}_{3h}$ point symmetry, which can rotate and vibrate, well reproduce the experimental spectrum of ^{12}C [6]. In contrast, an *ab initio* lattice approach using chiral effective field theory succeeded in reproducing the excitation energy of the Hoyle state [7]. Here, it is calculated to possess a "bent-arm" configuration. Furthermore, fermionic molecular dynamics (FMD) and antisymmetrized molecular dynamics (AMD) calculations predict a dominant ^{8}Be + α configuration [8,9].

It is also possible that the bosonic nature of the α particle dominates, meaning that the Hoyle state could be the nuclear analogue of atomic Bose Einstein condensation [10,11]. Models that limit the fermionic degrees of freedom of the α clusters successfully reproduce the charge form factor for electron inelastic excitation to the Hoyle state [12].

A potentially sensitive probe into the structure of the Hoyle state is to examine the ways that it decays into three α particles. It may break up through a sequential process, where an α particle is emitted, leaving ^{8}Be in its ground state, or through a direct decay process where the three α particles share the decay energy in a more complicated way. Quantifying the likelihood of the direct decay and the energy distribution of the three emitted α particles may lead

to an understanding of their initial configuration in the nucleus [13].

Recent experimental efforts have placed an upper limit on the direct decay contribution at 0.2% [14,15]. Here, we report an improvement on the upper limit for the direct 3α decay from the Hoyle state via a measurement of the ^{12}C(^{4}He, 3α)α reaction. A total of 9.3×10^4 Hoyle state decays were measured, increasing our sensitivity to the rare direct decay branch. A novel detector geometry was implemented in order to remove the dominant experimental background.

The present experimental measurements were performed using the MC40 cyclotron accelerator at the University of Birmingham, producing a ^{4}He^{2+} beam with a kinetic energy of 40 MeV, incident on a 100 μg cm^{-2} natural carbon target. An average beam current of 6 enA was used and data were acquired for a total of 60 hours. The Hoyle state was populated through the inelastic scattering channel, resulting in the overall break-up reaction of ^{12}C(^{4}He, 3α)α. To reduce the energy loss of the reaction products, the target was rotated by 40° with respect to the beam. The experimental setup is detailed in Fig. 1. An array of six *Micron W1* double-sided silicon strip detectors (DSSDs) were used to detect the charged reaction products on an event by event basis [Micron Semiconductor Ltd]. Each DSSD had a total surface area of 5×5 cm^2 and allowed both the energy and the direction of a particle to be determined. This enabled the momentum vector of each detected particle to be calculated, assuming each to be an α particle. The detector channels were calibrated in energy using a mixed ^{239}Pu, ^{241}Am, and ^{244}Cm α-particle source and had a typical energy resolution of 35–40 keV.

The detectors were positioned to maximize the efficiency for detecting all four final state reaction products (complete kinematics). A ΔE-E particle identification (PID) telescope consisting of 65 μm and 500 μm detectors was placed at a large scattering angle of 90° to detect the scattered beam particle. It covered scattering angles from −73° to −108°. At a center angle of 30°, the four remaining 500 μm DSSDs
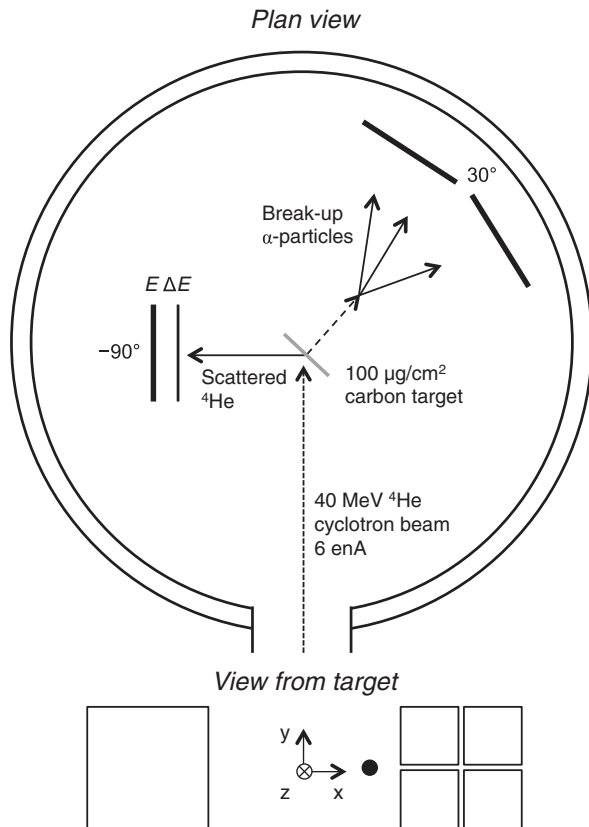
Plan view

FIG. 1.   Schematic drawing of the reaction chamber and detector positions along with an illustration of the break-up process.

FIG. 2.   Excitation energy spectrum of ^{12}C calculated from the three break-up α particles. Events are chosen where each α particle is detected in a separate DSSD. A total of 2.4×10^4 events are plotted. The points depict experimental data and the solid line shows the results of Monte Carlo simulations. The inset uses a logarithmic scale for a closer examination of the background.

were arranged in a quadrant formation in order to detect the three α particles resulting from the decay of the recoiling ^{12}C. A total angular coverage from 10° to 53° was achieved.

This arrangement permitted each detected α particle to strike a separate DSSD quadrant. If multiple particles with similar energies strike the same detector, this provides some ambiguity regarding their hit positions. This leads to an intractable experimental background, which is discussed in the most recent measurement of the direct decay branch [15]. Here, we remove this ambiguity, leading to almost background-free spectra. In the analogue processing electronics, a multiplicity condition of three hits on the quadrant arrangement, in coincidence with a single hit in the telescope, was demanded as a trigger for each valid event.

The reconstructed kinematics of the three α particles from the breakup were used to infer the excitation energy of the parent ^{12}C nucleus and to determine the decay mechanism. Two subsets of data were considered in the analysis; events where each α particle strikes a different DSSD and events where two strike the same detector. Ultimately, both subsets were used together to calculate the direct decay branch.

Figure 2 shows the measured ^{12}C excitation spectrum, calculated from the three break-up α particles. The 7.65 MeV Hoyle state was strongly populated. The condition that each particle was detected in a separate DSSD
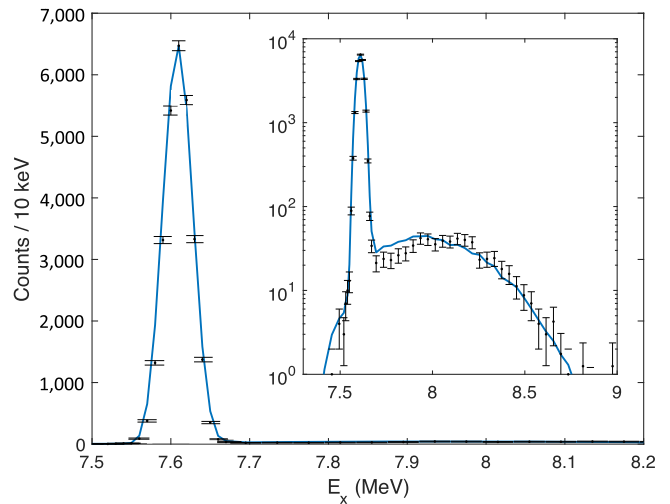
was applied and a cut on the Q value of each event was placed prior to plotting this spectrum. The results of Monte Carlo simulations of the reaction process including the detector geometry, experimental resolution, and backgrounds are also plotted as the solid line in Fig. 2. Details of the Monte Carlo code can be found in Refs. [16,17]. The simulations well reproduce the 42 keV peak width (FWHM) and the background profile by event mixing. The tail of the broad 0^+ resonance at 10.3 MeV will also contribute to background counts in this region.

Background suppression was achieved by placing cuts on the total momenta in each Cartesian direction and by demanding that the excitation energy calculated by the scattered ^{4}He ion matched that calculated from the three break-up α particles. A cut on the peak in Fig. 2 allowed decays from the Hoyle state to be cleanly examined. With these software gates, only 0.03% of mixed events reach the final spectra.

By measuring the energies and angles of the three break-up α particles, their energies in the center-of-mass frame of the decaying ^{12}C were determined. The relative energies of these particles are a reflection of the decay process in which they were produced. In a sequential decay, the first emitted α particle has a fixed energy dictated by the masses of the α and ^{8}Be fragments. This corresponds to approximately 1/2 of the total 3α break-up Q value. The remaining energy is shared between the two α particles from the decay of ^{8}Be.

If the decay instead proceeds through a direct process there are no such constraints, provided that energy and momentum are conserved. We consider three direct decay mechanisms: the particles are emitted collinear (DDL), the

three particles separate with similar energies (DDE), and the particles decay randomly to the available phase space (DDΦ). It has been proposed that the propensity for ^{12}C to decay through each of these mechanisms can lead to an understanding of its structure [13]. Sequential decays to the low energy tail of the ^{8}Be 2^{+} state could also contribute data that seem nonsequential. However, the additional angular momentum barrier will suppress this channel. Furthermore, the ^{8}Be ground state ghost anomaly only contributes at the level of 6×10^{-5} in this reaction channel [14,18]; below the sensitivity of the experiment.

The α-particle energies are best visualized using the symmetric Dalitz plot shown in Fig. 3 [19]. If ϵ_i is the fractional energy of the ith α particle (in the ^{12}C center-of-mass frame), the coordinates of the Dalitz plot are given by

$$x = \frac{\sqrt{3}}{2}(\epsilon_2 - \epsilon_1), \qquad y = \frac{1}{2}(2\epsilon_3 - \epsilon_1 - \epsilon_2). \quad (1)$$

In this coordinate system, if the decay proceeded through a sequential process, the data are required to lie on a triangular locus. This corresponds to the case that either ϵ_1, ϵ_2, or ϵ_3 are approximately equal to $1/2$. The 18 keV width of the triangle is due to the experimental resolution; the dominant contribution is the angular granularity of the DSSDs. The excellent resolution is obtained without the requirement for kinematic fitting [14]. Conservation of energy and linear momentum constrains the data to lie within a circle of radius $1/3$, marked in Fig. 3.

The majority of data points lie on the triangular locus, signifying a dominant sequential decay mechanism. To quantify the relative contributions of sequential and direct
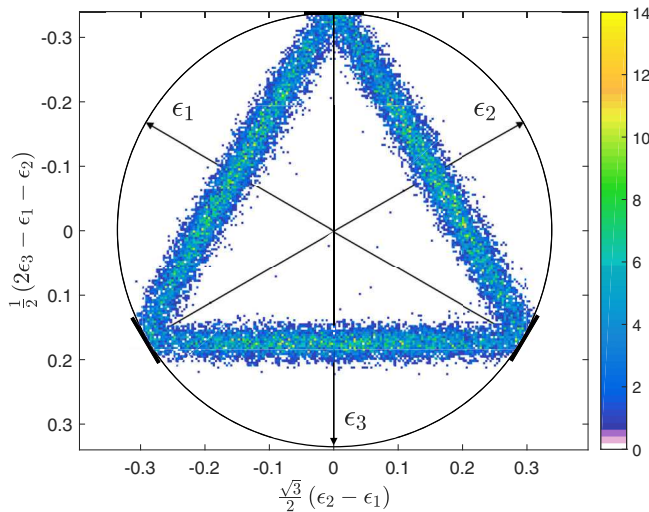
decay, it is necessary to fold and project Fig. 3 into a one-dimensional plot. Folding the Dalitz plot along each of its symmetry axes results in the data occupying a single sextant of the Dalitz plot. The results are shown in Fig. 4(a). Figure 4(b) shows the Monte Carlo simulation of the sequential decay process for the case where each particle strikes a separate DSSD. The data corresponding to where two α particles are permitted to strike the same DSSD are plotted in Fig. 4(c). Figure 4(d) shows the simulation for the uniform DDΦ direct decay process. The resulting nonuniformity is due to the detector acceptance.

The folded Dalitz plots were projected onto the vertical axis. The resulting one-dimensional plots contain a single peak at $\epsilon \approx 1/2$. These were fit with the simulated data in order to determine the relative sequential and direct decay components. The two subsets of data shown in Figs. 4(a) and 4(c) were fit simultaneously. Several fits are shown in Fig. 5. The lines represent the fit corresponding to various levels of the DDΦ direct decay branching ratio. The sequential decay mechanism provides a good fit to the experimental data without the requirement for any direct decay contribution. The tails of the distribution are well reproduced by the simulated background. With the normalization of equal counts in the experimental and simulated spectra, χ^2 per degree of freedom is equal to 1.08 (close to 50% confidence level).
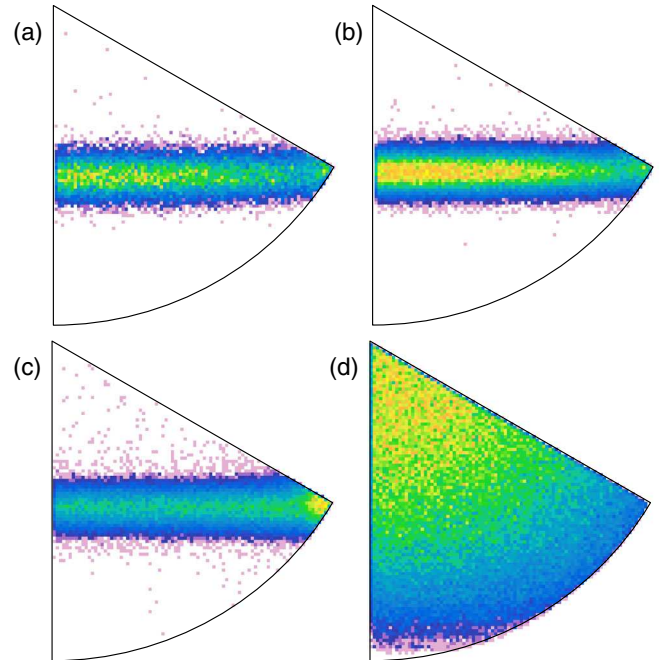

FIG. 4. Folded symmetric Dalitz plots. (a) Experimental data corresponding to three hits in separate DSSDs (2.4×10^4 events). (b) Monte Carlo simulation of the sequential decay process (1.1×10^5 events). (c) Experimental data corresponding to events where two particles strike the same DSSD (6.9×10^4 events). (d) Monte Carlo simulation of the DDΦ direct decay process (2.6×10^5 events).

FIG. 3. Symmetric Dalitz plot. This shows 2.4×10^4 Hoyle state break-up events, corresponding to the case where each α particle was detected by a separate DSSD. Sequential decay events are forced to lie on the triangular locus.
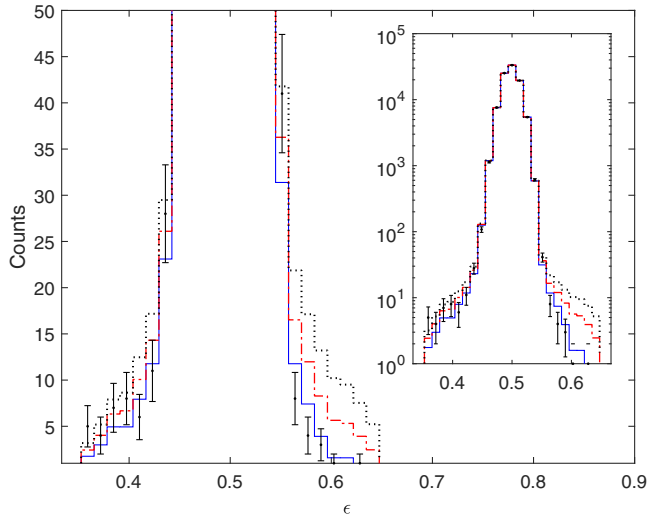
FIG. 5.   The projected Dalitz plot fractional energy spectrum. Points show all experimental data and the lines are the results of Monte Carlo simulations. The full spectrum is shown on a logarithmic scale as the inset and the main panel focuses on the tails of the distribution. The solid line, dot-dashed and dotted lines show simulations with a DDΦ contribution at 0%, 0.05%, and 0.1% respectively.

Limits were placed on the direct decay component by calculating the likelihood of reproducing the experimental data given a particular branching ratio. From the likelihood functions, the 2σ (95%) confidence intervals were separately calculated for the three direct decay mechanisms. We can *reject the direct decay* of the Hoyle state at the levels DDΦ > 0.047%, DDE > 0.026%, DDL > 0.004%.

A total of 9.3×10^4 events were considered, approximately 5 times more than any previous experiment. Further, the experimental background in Figs. 4(a) and 4(c) is lower than past experiments. As a result, the upper limit on DDΦ is over half an order of magnitude lower than the 0.2% obtained by Itoh *et al.* [15].

The confidence belt construction of Ref. [20] was also applied to the data. This approach solves the problem that the choice of upper limit or two-sided intervals may actually lead to incorrect confidence intervals, if the choice is based on the experimental data. This method also avoids unphysical confidence intervals, which in this case would correspond to negative branching ratios. For the DDΦ mechanism, this method gave the same results as are quoted above. The calculated DDE and DDL upper limits were different at 0.036% and 0.024%, respectively.

A Bayesian alternative to null-hypothesis significance testing was also performed based on Ref. [21]. Prior distributions based on the existing knowledge about this branching ratio were chosen [15]. However, since the present experimental measurements are of considerably higher precision than previous efforts, any objective prior distribution of the branching ratio had no effect on the calculated limits at the quoted level of precision.

This significant reduction in the upper limit for the direct decay branching ratio is important because it brings the upper limit for direct decay down to a level that is comparable with existing theoretical predictions [22]. In this sense, the present experimental results could provide an insight into the structure of the Hoyle state.

In a simple picture, the relative phase spaces for direct 3α and sequential $\alpha + {}^8$Be decays dominate the calculation of the branching ratio [23]. By considering the magnitude of the phase spaces for each decay type, with all other factors considered equal, the direct decay channel contributes just 0.18% of the total. In addition to the phase space, transmission probabilities through the Coulomb barrier for the decay will also come into play. To calculate this, semiclassical WKB calculations using the methods of reference [24] were performed. By Monte Carlo sampling the available phase space, the Coulomb barrier transmission probabilities were evaluated, and the branching ratio was calculated to be 0.06%. The observed experimental enhancement of the ^{8}Be $+ \alpha$ channel, compared with this calculation, could indicate that the α-condensate interpretation of the state is less likely to be correct. If the Hoyle state is a structureless α gas or condensate, then the decay should have equal probabilities for all of the possible partitions involving α-condensed subsystems [25]. However, the width of the Hoyle state has previously been calculated to be around 60 eV using the WKB approximation [26]. This is 3 times larger than the full computation and about 7 times larger than the experimentally measured value of 8.5 eV [27]. Therefore, it is difficult to form a meaningful comparison between this calculated branching ratio of 0.06% and the current experimental results.

Furthermore, Ishikawa performed a detailed theoretical analysis into the decay of the Hoyle state, calculated in the Faddeev three-body formalism [22]. The Hoyle state was considered to be a system of three interacting α particles. Each was treated as a boson and the complications arising due to their underlying four-nucleon fermionic structures were considered to be incorporated into the various α-α interaction potentials used. The break-up amplitude was calculated as a function of the momenta of the outgoing α particles and the form of the resulting Dalitz plot was predicted. This work concluded that the direct decay should contribute at a level $< 1\%$. Although the 0.047% limit extracted from the present experimental data lies below this theoretical prediction, this quoted direct decay contribution does not have sufficient precision to be compared with the experimental results. Further theoretical input is needed.

The resolution achieved in the present experiment has reached the limits of conventional charged-particle spectroscopy with realistic beam times. In order to examine the nature of the α energy distributions in more detail, another approach would be needed. With appropriate development the use of an optical time projection chamber (OTPC) [28] is one such promising tool.

To summarize, a significantly improved upper limit on the direct 3α decay of the Hoyle state has been experimentally measured. The upper limit now lies at a value that is similar to theoretical predictions, though future work is encouraged in order for a meaningful comparison to be made.

---

[*]robinsmith4@hotmail.co.uk

[†]t.kokalova@bham.ac.uk

[1] M. Freer, Rep. Prog. Phys. **70**, 2149 (2007).

[2] M. Freer, Nature (London) **487**, 309 (2012).

[3] L. R. Buchmann and C. A. Barnes, Nucl. Phys. **A777**, 254 (2006).

[4] F. Hoyle, Astrophys. J. Suppl. Ser. **1**, 121 (1954).

[5] M. Freer and H. O. U. Fynbo, Prog. Part. Nucl. Phys. **78**, 1 (2014).

[6] D. J. Marin-Lambarri, R. Bijker, M. Freer, M. Gai, Tz. Kokalova, D. J. Parker, and C. Wheldon, Phys. Rev. Lett. **113**, 012502 (2014).

[7] E. Epelbaum, H. Krebs, D. Lee, and Ulf-G. Meissner, Phys. Rev. Lett. **106**, 192501 (2011).

[8] M. Chernykh, H. Feldmeier, T. Neff, P. von Neumann-Cosel, and A. Richter, Phys. Rev. Lett. **98**, 032501 (2007).

[9] Y. Kanada-En'yo, Prog. Theor. Phys. **117**, 655 (2007).

[10] A. Tohsaki, H. Horiuchi, P. Schuck, and G. Röpke, Phys. Rev. Lett. **87**, 192501 (2001).

[11] Y. Funaki, H. Horiuchi, W. von Oertzen, G. Ropke, P. Schuck, A. Tohsaki, and T. Yamada, Phys. Rev. C **80**, 064326 (2009).

[12] Y. Funaki, A. Tohsaki, H. Horiuchi, P. Schuck, and G. Röpke, Eur. Phys. J. A **28**, 259 (2006).

[13] Ad. R. Raduta et al., Phys. Lett. B **705**, 65 (2011).

[14] O. S. Kirsebom et al., Phys. Rev. Lett. **108**, 202501 (2012).

[15] M. Itoh et al., Phys. Rev. Lett. **113**, 102501 (2014).

[16] N. Curtis et al., Phys. Rev. C **51**, 1554 (1995).

[17] N. Curtis et al., Phys. Rev. C **53**, 1804 (1996).

[18] F. C. Barker and P. B. Treacy, Nucl. Phys. **38**, 33 (1962).

[19] R. H. Dalitz, Philos. Mag. **44**, 1068 (1953).

[20] G. J. Feldman and R. D. Cousins, Phys. Rev. D **57**, 3873 (1998).

[21] J. L. Puga, M. Krzywinski, and N. Altman, Nat. Methods **12**, 377 (2015).

[22] S. Ishikawa, Phys. Rev. C **90**, 061604 (2014).

[23] Geant4 International Collaboration, Geant4 10.3 Physics Reference Manual, Chap. 37, p. 483, http://geant4.cern.ch/support/userdocuments.shtml.

[24] E. Garrido, D. V. Fedorov, A. S. Jensen, and H. O. U. Fynbo, Nucl. Phys. **A748**, 27 (2005).

[25] Tz. Kokalova, N. Itagaki, W. von Oertzen, and C. Wheldon, Phys. Rev. Lett. **96**, 192502 (2006).

[26] E. Garrido, D. V. Fedorov, A. S. Jensen, and H. O. U. Fynbo, Nucl. Phys. **A748**, 39 (2005).

[27] F. Ajzenberg-Selove, Nucl. Phys. **A506**, 1 (1990).

[28] W. R. Zimmerman et al., Phys. Rev. Lett. **110**, 152502 (2013).